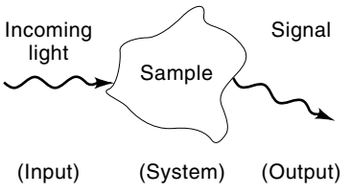

Figure 1. Optical signal as the result of interaction of an electromagnetic wave with the sample.

OPTICAL PROPERTIES

Materials science may be characterized by a tremendous diversity of techniques, including mechanical characterization, electrical methods, chemical analysis, electron microscopy, and others. This article presents an introduction to the *optical characterization* of solid state materials.

In the framework of classical electrodynamics, any kind of light (which is used in optics) may be regarded as a superposition of electromagnetic waves. The idea of optical material characterization is quite simple: If we have an object to be investigated (a *sample*), we have to bring it into interaction with electromagnetic waves (light). As the result of the interaction with the sample, certain properties of the light will be modified. The specific modification of the properties of electromagnetic waves resulting from the interaction with the sample should give us information about the nature of the sample of interest.

For sufficiently low light intensities, the interaction process does not result in sample damage. Therefore, the majority of optical characterization techniques belongs to the nondestructive analytical tools in materials science. This is one of the advantages of optical methods.

Although the main idea of optical characterization is quite simple, it may be an involved task to turn it into practice. In fact, one has to solve two problems. The first one is of an entirely experimental nature: The modifications in the light properties (which represent our *signal*) must be detected. For standard tasks, this part of the problem may be solved with the help of commercially available equipment. The second part is more closely related with mathematics: From the signal (which may be simply a curve in a diagram) one has to conclude on concrete quantities characteristic for the sample. Despite the researcher's intuition, this part may include severe computational efforts. Thus, the solution of the full problem requires the researcher to be skilled in experiment and theory as well.

Let us now have a look at Fig. 1. Imagine the very simplest case—a monochromatic light wave impinging on a sample which is to be investigated. The parameters characterizing the incoming light (wavelength, intensity, polarization of the light, propagation direction) are supposed to be known. Further imagine that as the result of the interaction with the sample, we are able to detect an electromagnetic wave with modified properties. With properties of the electromagnetic wave may have changed as the result of the interaction with the sample? In principle, all of them may have changed. It is possible that the interaction with the sample leads to changes in the wavelength of the light. Typical examples are provided by Raman scattering, or by several nonlinear optical processes. The polarization of the light may change as well. Ellipsometric techniques detect polarization changes and use them to judge the sample properties. Clearly, the light intensity may change (in most cases the light will be attenuated). This gives rise to numerous photometric methods analysing the sample properties based on the measurement of intensity changes. And finally, we know that the refraction of light may lead to changes in the propagation direction. Any refractome-

J. Webster (ed.), *Wiley Encyclopedia of Electrical and Electronics Engineering*.

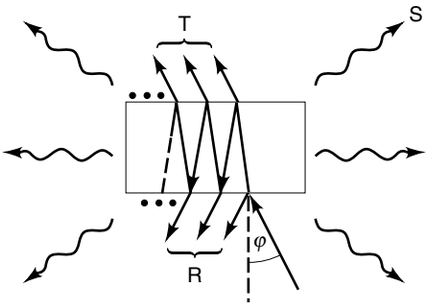

Figure 2. The optical signal may be generated by transmitting (T), specularly reflecting (R), or scattering (S) the incident light. φ is the angle of incidence.

ter makes use of this effect to determine the refractive index of a sample.

The diversity of parameters characterizing electromagnetic radiation (in practice they are more than those mentioned here) may give rise to quite diverse optical characterization techniques. Clearly, in the framework of this paper only a few of them may be discussed.

Any practical situation is more complicated than that shown in Fig. 1. After interaction with the sample, light may leave the sample in several directions (Fig. 2). From the phenomenological point of view, the light may either be

- *Transmitted* through the sample (in a well-defined direction), or
- *Specularly reflected* from the sample, or
- *Diffusely scattered* at the sample surfaces or in its volume, or
- *Absorbed at the sample* surfaces or in its volume

Let us for simplicity focus on the intensities of the signals. It is a common practice to define the *transmittance* T of the sample as the ratio of the intensity of the transmitted light and that of the incoming light (1). Accordingly, we define the *specular reflectance* R as the ratio of the specularly reflected intensity and the incoming one. If we deal with a sample that does neither diffusely scatter nor absorb the irradiation, then the thus defined transmittance and reflectance must sum up to the value one—simply as a result of the energy conservation law. In practice, a certain fraction of the light intensity is diffusely scattered. That leads us to the definition of the optical *scatter* S as the ratio of the intensity of the light participating in scattering processes and the incoming intensity. Analogously, we define the *absorptance* A as the ratio of the absorbed intensity and the incoming one. In the presence of absorption and scatter, the energy conservation law may be written as

$$T + R + A + S = 1 \tag{1}$$

So that these four quantities are not independent from each other, and accurate knowledge of three of them allows the fourth to be immediately calculated. Nevertheless, all four quantities T, R, S, and A may, in principle, be measured independently from each other. The algebraic sum of absorption and scatter is often called *optical loss*, and the measurement of the optical loss represents one of the most challenging experimental tasks of optical material characterization (2).

Let us make a final remark in this context. The values T, R, S, and A are characteristic for a sample in specific experimental conditions. This means that both sample material and its geometry (including the experiment geometry) are responsible for the signal. If one is interested in the pure material properties, the geometrical influences on the signal have to be eliminated, experimentally or by calculations.

Important Spectral Regions

Table 1 provides an overview on important spectral regions and the origin of characteristic material absorption structures (3,4).

LIGHT PROPAGATION IN CLASSICAL PHYSICS

The Wave Equation in the Homogeneous and Isotropic Case

In terms of classical physics, the propagation of electrodynamic waves may be described starting from Maxwell's equations (5,6). In order to simplify the description here, we restrict ourselves to optically homogeneous and isotropic media. Furthermore, we will regard the medium as nonmagnetic. In this case, Maxwell's equations lead to

$$\text{rotrot}\boldsymbol{E} \equiv \text{graddiv}\boldsymbol{E} - \Delta\boldsymbol{E} = -\mu_0 \frac{\partial^2}{\partial t^2}\boldsymbol{D} \tag{2}$$

Table 1. Important Spectral Regions

Spectral Region	Vacuum Wavelength λ (nm)	Wavenumber $v = 1/\lambda$ (cm^{-1})	Angular Frequency $\omega = 2\pi vc$ (s^{-1})	Photon Energy $W = hcv$ (eV)	Origin of Absorption (Examples)
Far Infrared (FIR)	$10^6 - 5 \times 10^4$	$10 - 200$	$1.9 \times 10^{12} - 3.8 \times 10^{13}$	$1 \times 10^{-3} - 2 \times 10^{-2}$	Free carriers; orientation
Middle Infrared (MIR)	$5 \times 10^4 - 2.5 \times 10^3$	$200 - 4000$	$3.8 \times 10^{13} - 7.5 \times 10^{14}$	$2 \times 10^{-2} - 5 \times 10^{-1}$	Free carriers; vibrations
Near Infrared (NIR)	$2.5 \times 10^3 - 8 \times 10^2$	$4000 - 12500$	$7.5 \times 10^{14} - 2.4 \times 10^{15}$	$5 \times 10^{-1} - 1.6$	Free carriers; vibrational overtones
Visible (VIS)	$8 \times 10^2 - 4 \times 10^2$	$12500 - 25000$	$2.4 \times 10^{15} - 4.7 \times 10^{15}$	$1.6 - 3.1$	Excitation of valence
Ultraviolet (UV)	$4 \times 10^2 - 10$	$25000 - 10^6$	$4.7 \times 10^{15} - 1.9 \times 10^{17}$	$3.1 - 124$	Electrons
X-ray (X)	$10 - 0.005$	$10^6 - 2 \times 10^9$ (unusual)	$1.9 \times 10^{17} - 3.8 \times 10^{20}$	$124 - 25000$	Excitation of core electrons

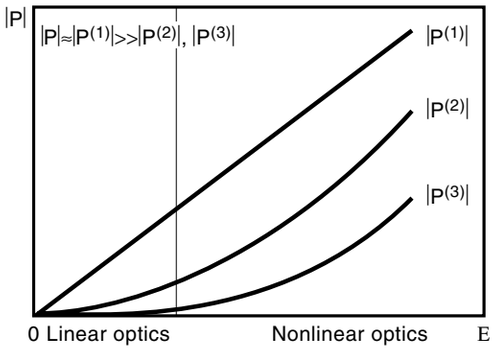

Figure 3. The polarization of a medium as a function of the electric field strength contains linear as well as nonlinear contributions. For weak electric fields, the linear contribution is dominant, thus determining the field of linear optics.

with $\boldsymbol{E}$ the vector of electric field strength, and $\boldsymbol{D}$ that of the induction. Per definition, the induction is connected with the electric field via

$$\boldsymbol{D} = \epsilon_0 \boldsymbol{E} + \boldsymbol{P} \tag{3}$$

where $\boldsymbol{P}$ is the so-called polarization of the medium. It is defined as the dipole moment per volume. From the viewpoint of optical material characterization, it plays the key role here because it contains the specific optical properties of the medium where the electromagnetic wave will propagate. Combining Eq. (2) and Eq. (3), we obtain

$$\text{graddiv}\boldsymbol{E} - \Delta\boldsymbol{E} + \mu_0\epsilon_0\frac{\partial^2}{\partial \mathrm{t}^2}\boldsymbol{E} = -\mu_0\frac{\partial^2}{\partial \mathrm{t}^2}\boldsymbol{P} \tag{4}$$

Equation (4) completely describes the propagation of electromagnetic waves in a homogeneous, isotropic, and nonmagnetic medium. It is now essential to define a relationship between $\boldsymbol{E}$ and $\boldsymbol{P}$ to solve Eq. (4). Considering only induced (by the field) dipole moments, an arbitrary dependence $\boldsymbol{P(E)}$ may be formally written as Taylor's sum (7,8):

$$\boldsymbol{P} = \boldsymbol{P}^{(1)} + \boldsymbol{P}^{(2)} + \boldsymbol{P}^{(3)} + \cdots \tag{5}$$

with

$$P^{(1)} \propto E, P^{(2)} \propto E^2, P^{(3)} \propto E^3, \ldots \tag{6}$$

and so on. The principal E-dependence of these terms is illustrated in Fig. 3 (9). From Fig. 3 it is essential to remark that for weak field strength values the polarization must be dominated by the first (linear) term in Eq. (5). In this field strength region, Eq. (4) may be solved regarding the simple dependence

$$\boldsymbol{P} \approx \boldsymbol{P}^{(1)} \propto \boldsymbol{E} \tag{7}$$

Then Eq. (4) describes the processes of the so-called *linear optics*. The more general case [Eqs. (5, 6)] is called *nonlinear optics*. In the forthcoming, we will focus on the linear case.

Dispersion of Optical Constants

Let us now postulate the final form of the relation Eq. (7), valid for linear optics. The polarization at the moment t in the point characterized by the vector $\boldsymbol{r}$ may be written as

$$\boldsymbol{P}(\mathrm{t}, \boldsymbol{r}) = \epsilon_0 \int_0^\infty d\tau \int_\mathrm{V} \kappa(\tau, \boldsymbol{R})\boldsymbol{E}(\mathrm{t} - \tau, \boldsymbol{r} - \boldsymbol{R})\, \mathrm{d}\boldsymbol{R} \tag{8}$$

Equation (8) may be understood in the following way: The polarization (at the time t in the point $\boldsymbol{r}$), which represents the response of a system on the stimulating field, may depend on

- The spatial field strength distribution in the volume V surrounding the point of interest
- At all *previous* moments (causality principle)
- The specifics of the medium, which are hidden in the response function κ

The combination of Eq. (4) and Eq. (8) may be satisfied by a transversal propagating wave according to

$$\boldsymbol{E}(\mathrm{t}, \boldsymbol{r}) = \boldsymbol{E}_0 e^{-\mathrm{i}(\omega \mathrm{t} - \boldsymbol{kr})} \tag{9}$$

This may be checked substituting Eq. (8) and Eq. (9) into Eq. (4). One will then find that Eq. (9) indeed is a solution of Eq. (4) and Eq. (8), if the absolute value of the wavevector $\boldsymbol{k}$ is equal to

$$-k^2 + \mu_0\epsilon_0\epsilon\omega^2 = 0 \Rightarrow k = \pm\sqrt{\epsilon}\frac{\omega}{c} = \pm\sqrt{\epsilon}\frac{2\pi}{\lambda} \tag{10}$$

where the value ϵ is called the *dielectric function* of the medium and must satisfy

$$\epsilon = \epsilon(\omega, \boldsymbol{k}) = 1 + \int_0^\infty d\tau \int_V \kappa(\tau, \boldsymbol{R}) e^{i(\omega\tau - \boldsymbol{kR})}\, d\boldsymbol{R} \tag{11}$$

From our treatment it turns out that the introduced dielectric function

- Has to be regarded as a complex function, and consequently has a real and an imaginary part
- May depend on the frequency of the electric field. This effect is called time dispersion or frequency response
- May depend on the wavevector $\boldsymbol{k}$ (and therefore on the wavelength of the light). The latter effect is called spatial dispersion or wavelength response

While time dispersion occurs, when the light frequency comes close to a characteristic eigen-frequency of the medium investigated, spatial dispersion will be found when the light wavelength equals a characteristic spatial dimension of the medium. In materials science practice, spatial dispersion is often negligible, and we will concentrate on the time dispersion often simply called dispersion in the forthcoming section. Keeping in mind these remarks, we finally obtain from Eq. (9)

$$\boldsymbol{E}(\mathrm{t}, \boldsymbol{r}) = \boldsymbol{E}_0 \mathrm{e}^{-\mathrm{Im}\sqrt{\epsilon}\frac{\omega}{\mathrm{c}}\mathrm{r}} e^{-\mathrm{i}(\omega \mathrm{t} - \mathrm{Re}\sqrt{\epsilon}\frac{\omega}{\mathrm{c}}\mathrm{r})} \tag{12}$$

which represents an attenuated wave if the imaginary part of the square root of the dielectric function is positive. This leads us to the definition of the *absorption coefficient* α:

$$\alpha(\omega) = 2\frac{\omega}{c}\mathrm{Im}\sqrt{\epsilon(\omega)} \tag{13}$$

It is given in reciprocal centimeters, where its inverse value represents the penetration depth of light into matter. On the contrary, the real part of $\sqrt{\epsilon}$ affects the phase velocity of the light. We define the dimensionless *refractive index* n via

$$n(\omega) = \mathrm{Re}\sqrt{\epsilon(\omega)} \tag{14}$$

As a result of the dispersion of ϵ, both the refractive index and the absorption coefficient are frequency dependent.

The refractive index and the absorption coefficient are a pair of so-called optical constants (characteristic for a given medium), that completely describe the process of wave propagation within a homogeneous and isotropic medium. Alternatively, often the complex refractive index N is defined

$$N(\omega) = n(\omega) + iK(\omega) = \sqrt{\epsilon(\omega)} \tag{15}$$

Its real part describes the phase velocity of the wave (and consequently the refraction), and its imaginary part (often: *extinction index*) the attenuation.

The frequency dependence of the optical constants is closely related to the frequency dependence of the corresponding sample spectra. Generally, in optical spectra theory, there exist two different tasks. The first one is the calculation of spectra, when the optical constants and the system geometry are known. This kind of calculation is called a forward search, and in many situations this may be accomplished in terms of explicit formulae. The second one is what we often have in practice: The spectra are known (they have been measured), and the optical constants have to be calculated. This so-called reverse search is a much more complicated procedure, because usually no explicit formulae allow the calculation of optical constants from the spectra. The typical way is to perform forward calculations with different assumed sets of optical constants, until one of the thus generated spectra fits the experimental one. In this sense the reverse search strategy bases on forward search calculations. It is therefore essential to start our further discussion with examples of spectra calculations. We will then describe a few basic experimental techniques before coming to the question of reverse search procedures.

Interfaces

Up to now we have dealt with the description of a light wave within a homogeneous and isotropic medium. As already suggested from Fig. 2, the surfaces and interfaces of the sample will however play an important role for transmission and reflection processes. The influence of an interface may be mathematically taken into account introducing electrical field transmission and reflection coefficients according to (see Fig. 4)

$$t = \frac{E_t(z=0)}{E_e(z=0)}; \quad r = \frac{E_r(z=0)}{E_e(z=0)} \tag{16}$$

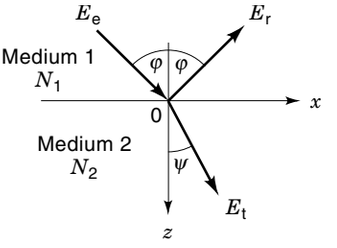

Figure 4. Incident (e), transmitted (t), and reflected (r) beam at a smooth interface. The z-axis is perpendicular to the interface.

In accordance with Fig. 4, φ is the incidence angle, and ψ that of refraction. In the following, medium 1 will *always* mark the medium from where the light is incident. The transmission and reflection coefficients are found to be polarization-dependent, where the subscript p denotes *parallel polarization* (the electric field vector is linearly polarized in the plane of incident beam and surface normal, which is the x–z plane in our description), while subscript s marks *perpendicular polarization* (electric field vector perpendicular to incident beam and surface normal). In these terms, the transmission and reflection coefficients are given by Fresnel's formulae (1):

p–Polarization:

$$r_p = \frac{N_2\cos\varphi - N_1\cos\psi}{N_2\cos\varphi + N_1\cos\psi}; \quad t_p = \frac{2N_1\cos\varphi}{N_2\cos\varphi + N_1\cos\psi}$$

s–Polarization:

$$r_s = \frac{N_1\cos\varphi - N_2\cos\psi}{N_1\cos\varphi + N_2\cos\psi}; \quad t_s = \frac{2N_1\cos\varphi}{N_1\cos\varphi + N_2\cos\psi} \tag{17}$$

$$\frac{\sin\varphi}{\sin\psi} = \frac{N_2}{N_1}$$

The combination of Eq. (12) and Eq. (17) allows the calculation of light propagation through homogeneous samples with smooth surfaces. As intensities are proportional to the square of the absolute values of the complex field amplitudes, the transmittance, the reflectance, and the absorption become accessible to calculations, if only the geometry of the sample (and illumination geometry), and all optical constants are known. Thus, for example, one may calculate the transmission and reflection spectra of a thick absorbing wafer (medium 2) with parallel smooth surfaces, embedded in a nonabsorbing environment (medium 1), taking into account all multiple internal reflections. In fact this is again the situation as shown in Fig. 2, and it allows an exact calculation of transmittance and reflectance. As a result of summarizing the intensities of all internal waves, one obtains the expressions (9)

$$T = \frac{|t_{12}|^2|t_{21}|^2 e^{-2\frac{\omega}{c}d\mathrm{Im}\sqrt{N_2^2-\sin^2\varphi}}}{1-|r_{12}|^2|r_{21}|^2 e^{-4\frac{\omega}{c}d\mathrm{Im}\sqrt{N_2^2-\sin^2\varphi}}};$$
$$R = |r_{12}|^2 + \frac{|t_{12}|^2|r_{21}|^2|t_{21}|^2 e^{-4\frac{\omega}{c}d\mathrm{Im}\sqrt{N_2^2-\sin^2\varphi}}}{1-|r_{12}|^2|r_{21}|^2 e^{-4\frac{\omega}{c}d\mathrm{Im}\sqrt{N_2^2-\sin^2\varphi}}} \tag{18}$$

Here, the r and t values are the Fresnel coefficients from Eq. (17), and d is the thickness of the wafer. The subscripts explain the direction of the wave (thus t_{12} means that the wave

transmits the interface coming from medium 1 and entering medium 2). The reflectance and transmittance are thus completely determined by the incidence angle, polarization, frequency, sample thickness, and optical constants. Because (up to now) in our assumptions scatter mechanisms have been excluded (homogeneous media, smooth surfaces), the bulk absorption loss may simply be calculated from T and R using Eq. (1) and neglecting S.

Equation (18) represent the simplest example of a forward search procedure, where the sample's properties (material, geometry) are known, as well as all parameters of the (optical) input (polarization, frequency, amplitude, propagation direction). From these data, the optical output (viz., transmittance and reflectance) are calculated.

For illustration, Figs. 5 and 6 demonstrate a set of optical constants as may be calculated from a multioscillator model, and the corresponding spectra obtained from Eq. (18) assuming normal incidence and a sample thickness of 0.1 mm. The dielectric function of the multioscillator model has been described by

$$\epsilon(\omega) = \text{const.} + \frac{1}{\pi}\sum_{j=1}^{5} J_j \left(\frac{1}{\omega_{0j} - \omega - i\gamma_j} + \frac{1}{\omega_{0j} + \omega + i\gamma_j} \right) \quad (19)$$

where the constant parameters J, ω_0, and γ have been chosen to model five mutually overlapping absorption lines in the MIR. Figure 5 shows the optical constants calculated via Eq. (13) and Eq. (14) assuming Eq. (19) for the dielectric function. The normal incidence spectra according to Eq. (18) are shown in Fig. 6 and demonstrate that the assumed absorption structure may well be identified from the spectra.

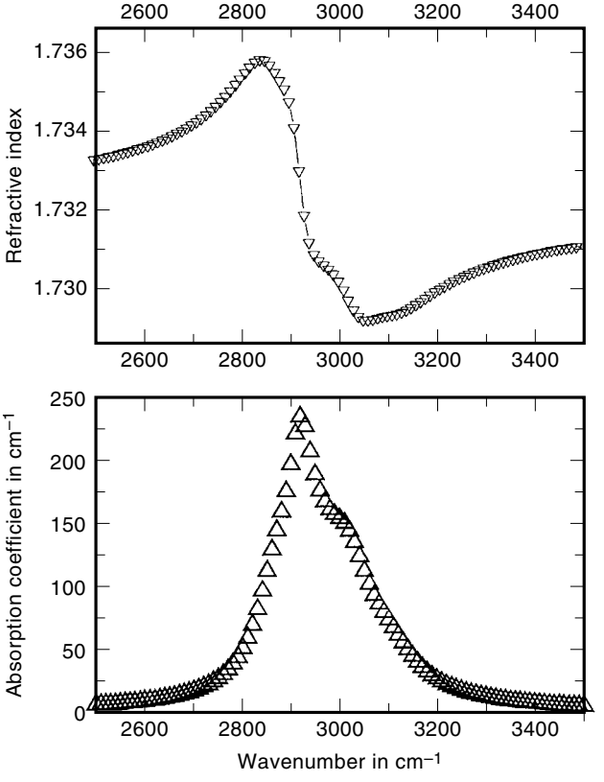

Figure 5. The frequency dependence of the refractive index and the absorption coefficient are strongly correlated to each other. This figure shows the refractive index (upper graph) and the absorption coefficient (lower) for the special case of a multioscillator model (see text). This model is frequently used to describe optical constants in the presence of single absorption lines.

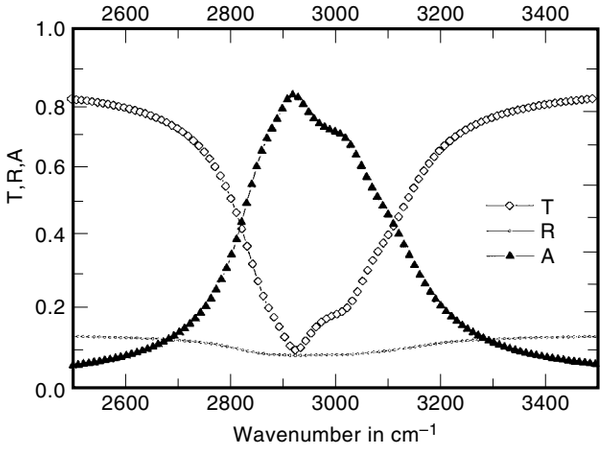

Figure 6. Transmittance, reflectance, and absorption (normal incidence) calculated for a 0.1 mm thick wafer according to Eq. (18). Optical constants as shown in Fig. 5. This is an example for a forward search procedure (spectra calculation). In such a sample, an absorption feature may clearly be identified from the transmission spectrum only.

The inclusion of scatter losses requires a refinement of our expressions. The scatter losses may occur at the surfaces and in the bulk. In many practically relevant cases, the surface scatter losses are dominant, because the optical constant discontinuities are usually larger at the surface than in the bulk inhomogeneities. However, for absorption losses we will assume that the surface absorption losses are negligible compared with the bulk losses. In experimental situations, where surface and bulk loss contribution are of the same order of magnitude, they may be separated from each other by investigating samples with different thickness values.

The simplest way to consider surface scatter losses in the equations for specular transmittance and reflectance is to multiply the Fresnel-coefficients with a roughness-dependent attenuation factor. For normal incidence, the corresponding formulae are:

$$\begin{aligned} t_{12} &\to t_{12} e^{-\frac{1}{2}\left[2\pi(n_1 - n_2)\frac{\sigma}{\lambda}\right]^2}; \\ r_{12} &\to r_{12} e^{-\frac{1}{2}\left[4\pi n_1 \frac{\sigma}{\lambda}\right]^2}; \\ r_{21} &\to r_{21} e^{-\frac{1}{2}\left[4\pi n_2 \frac{\sigma}{\lambda}\right]^2} \end{aligned} \quad (20)$$

Here, σ is the root mean square (rms) interface roughness. Clearly, with increasing roughness, the specular reflectance and transmittance are attenuated (and consequently, the scatter loss increases). Please note that surface roughness may decrease the specular reflectance down to zero, if the wavelength is sufficiently small. This is in contrast to the effects of bulk absorption, because the latter cannot depress the finite reflection signal from the first surface.

Measurements of Optical Loss

Today, transmission spectrophotometers belong to the standard equipment in many university and industrial labs. Typi-

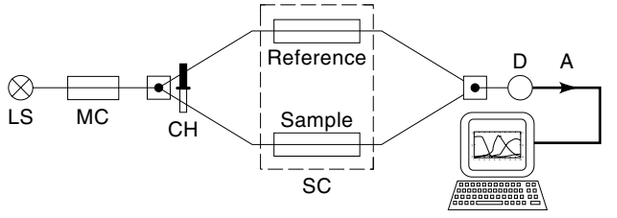

Figure 7. Principal scheme of a double beam dispersive spectrophotometer; (LS) light source, (MC) monochromator, (CH) chopper, (SC) sample compartment, (D) detector, (A) amplifier.

cal spectrophotometers are either designed for the UV/VIS region (UV/VIS spectrometer, which often work with spectrally dispersive monochromators as shown schematically in Fig. 7) or for the MIR (so-called IR spectrometers). IR spectrometers are produced today to an increasing extent as Fourier transform spectrometers. This has led to the abbreviation FTIR (Fourier transform infrared).

These spectrometers do not contain monochromators. Instead, a built-in interferometer (often of Michelson type) records the interferogram of the polychromatic light coming from the sample or a reference. From the intensity distribution in the interferogram, the spectrum of the incoming light may be calculated by means of a fast Fourier transformation (FFT) procedure. Thus, the output represents the same type of spectra (for example, transmittance) as supplied by a dispersive spectrophotometer. An important advantage of the FTIR technique is the much faster spectra registration.

The NIR region is usually accessible in so-called UV/VIS/NIR-dispersive spectrometers, or as an optional upgrading of FTIR spectrometers. The latter type of spectrometer also allows upgrading for FIR measurements.

In its standard version, a transmission spectrometer performs measurements of the transmittance with an absolute measurement error of approximately 0.002 to 0.01, depending on the quality of the spectrometer and the wavelength range. Usually, a suitable specular reflectance attachment is optionally available, so that T and R may be measured. From that, the optical loss may be calculated from Eq. (1) for the relevant light incidence geometry.

Particularly, one may design measurement situations where the transmittance completely vanishes. Examples are provided by IRAS (*infrared reflection absorption spectroscopy*) and ATR (*attenuated total reflection*). The first one has been developed to investigate the optical loss of thin adsorbate layers on metal substrates. As the metal substrate does not transmit light, the optical loss may be directly determined from the reflectance via Eq. (1). It may be shown from a detailed analysis of Fresnel's formula that the best sensitivity for *adsorbate absorption loss detection* demands the application of grazing incidence light with linear parallel polarization. Usually, the incidence angle is 85° or larger. The method is based on the specific behavior of the IR optical constants of metals, therefore its application is restricted to the IR, as indicated by its name.

Although the ATR method works in larger spectral regions, it assumes that the sample has a lower refractive index than the medium from where the light is incident. As a special conclusion from Fresnel's coefficients, the reflectance becomes 1 when both media 1 and 2 are nonabsorbing (purely real refractive indices), and the incidence angle satisfies the condition:

$$\sin\varphi \geq \frac{n_2}{n_1} \tag{21}$$

This situation is called total reflection of light. If, however, the refractive index of the sample has a nonvanishing imaginary part (lossy sample medium), then the reflectance decreases, and one speaks about attenuated total reflection. So one can calculate the sample material extinction index simply from the reflectance attenuation. In multiple reflection arrangements, ATR is a sensitive tool to determine small absorption losses (1).

The physical reason for the total reflection attenuation is the following: Even in ideal total reflection conditions the second medium is penetrated by a surface wave, which travels along the interface and damps quickly into the depth of the sample. In the geometry of Fig. 4, its electric field is proportional to the wave function:

$$e^{-i\left(\omega t-\frac{\omega}{c}n_1 x\sin\varphi\right)}e^{-\frac{\omega}{c}\sqrt{n_1^2\sin^2\varphi-n_2^2}z} \tag{22}$$

If the sample medium is lossy, then this surface wave needs to be permanently fed by the incident light, which leads to the detectable reflection attenuation.

Clearly, in any real situation, from the knowledge of two data (T and R) only the full optical loss may be determined. A discrimination between absorption and scatter losses is then impossible without additional model assumptions on the nature of the sample and their realization in refined mathematical spectra fitting procedures. An indication of surface scatter at the first sample surface may be drawn from the specular reflectance: If the first surface is rough, the specular reflectance gradually decreases down to zero with increasing frequency, in agreement with Eq. (20).

Another principal problem occurs in connection with the measurement of small loss values. As T and R are measured with a finite accuracy, the measurement of small losses (typically below 0.01) becomes impossible by this method. This is simply a consequence of the high under-ground signal, provided by the transmittance and the reflectance spectra. In such cases, one should directly measure the optical loss, and not conclude on it from T and R measurements (6,10).

Occasionally, corresponding attachments may also be combined with the previously mentioned spectrophotometers. Backscattering losses (back into medium 1) and forward scatter can be measured in so-called integrating sphere attachments, where the diffusely scattered light is collected and brought to the detector. Thus, a scatter signal integrated over all scattering angles is measured, and this signal is commonly called total integrated scatter (TIS). These spheres are commercially provided for the NIR/VIS/UV spectral regions (coated with $BaSO_4$ or Spectralon) or for the MIR (coated with Infragold). From the viewpoint of their size, these spheres reach from minispheres (a few centimeters in diameter) up to devices with more than one meter in diameter. As already mentioned, scatter losses may principally originate from the volume and the surfaces of the sample. In the case that the scatter loss originates only from one surface with a surface roughness σ, the latter may be determined from a measure-

ment of the diffuse backscatter loss and the specular reflectance. For small scatter losses, we obtain from Eq. (20):

$$\sigma = \frac{\lambda}{4\pi n_1}\sqrt{\frac{S_{(\text{back into medium 1})}}{R}} \tag{23}$$

The accurate measurement of *absorption losses* is based on the idea that the energy absorbed in the sample must either leave the sample (with a certain time delay) or enhance its temperature. In other words: The absorbed energy portion will participate in relaxation processes, and this is our chance to detect it. In order to detect very small absorption losses, absorption measurements are often accomplished with high incident light intensities, reliably supplied from laser sources.

The nature of the sample and its environmental conditions (e.g., temperature) will determine which of the relaxation channels works most rapidly. If radiative relaxation is fast enough, the fluorescence intensity allows us to conclude on the previously absorbed energy, and thus to determine the absorption. This is what is done by the *fluorescence method*. If nonradiative relaxation is faster, then the absorbed energy will finally lead to sample heating. As the temperature increase may be conveniently measured, the absorption of the sample may be determined. Thus we have *calorimetric methods* of absorption measurements. Other absorption measurement techniques make use of the sample heating without direct temperature measurements. Thus, the *optoacoustical measurements* detect the sound wave generated in a medium as a result of the absorption of pulsed light due to thermal expansion. Further methods detect the deformation of the sample surface, caused by thermal expansion due to light absorption. This deformation may be optically detected by the angular deflection of a weak probe beam. The corresponding method is called *photothermal deflection spectroscopy* (PDS). Alternatively, the thermal expansion of the embedding medium surrounding the sample surface may be detected through its refractive index change. If the probe beam is of grazing incidence, the refractive index gradient in the vicinity of the heated surface leads to an angular deflection of the probe beam, which may be detected.

SELECTED PROBLEMS OF OPTICAL CHARACTERIZATION

Reverse Search Procedures

In many cases, one is not only interested in a measurement of the optical loss, but in a more complete investigation of the optical properties of a sample and, in particular, of the optical properties of the sample material. The latter are hidden in its optical constants, so that the task may be to determine the optical constants of a medium from measured experimental spectra. In the simplest case this may be measurements of the transmittance and/or the reflectance. In other cases ellipsometric data are to be discussed. The general philosophy, however, does not depend on whether photometric or ellipsometric data or a combination of them are available.

As exemplified in the previous sections, it is possible to provide explicit expressions for the spectra of any sample if geometry and optical constants are known. A more complicated problem is the so-called *reverse search procedure*, where the spectra and more or less complete data on the geometry are given, and the optical constants of the medium are to be determined. Additionally, complementation of geometrical information (e.g., sample thickness) may be required.

It is often impossible to obtain explicit expressions for the optical constants as a function of the measured data [see, e.g., Eq. (18)]. This makes the numerical side of the reverse search more complicated than the forward search, because it may be necessary to apply involved iteration procedures to find the result. As a further complication, unambiguity and numerical stability of the result may not be guaranteed.

From the formal point of view, the reverse search procedures may be classified into single wavelength methods and multiwavelength methods (11). The latter include the Kramers–Kronig methods as well as curve-fitting techniques. Often, the reverse search bases on the numerical minimization of an appropriately defined error function F, for example:

$$F = \sum_{i=1}^{M}\sum_{j=1}^{Z} w_i(\omega_j)[\Phi_{i,\text{theor.}}(N(\omega_j), \omega_j, \ldots) - \Phi_{i,\text{measurement}}(\omega_j)]^{2g} \tag{24}$$

Here, M is the number of available experimental spectra $\Phi_{i,\text{measurement}}$, each containing Z values recorded at the angular frequency values ω_j. g is an integer, often $g = 1$. The $\Phi_{\text{i,theor.}}$ values represent theoretical expressions for the spectra, they are dependent on the concrete physical model chosen to describe the system. As examples, the expressions in Eq. (18) may be used, if a wafer with plane boundaries is investigated. The weighting functions w_i are usually inversely proportional to the corresponding measurement error at a power $2g$.

The numerical minimization of Eq. (24) represents a purely mathematical problem, and the corresponding skills will not be discussed here. In the ideal case, a set of optical constants may be found which generates theoretical spectra equal to those measured, so that F becomes zero. In practice this is impossible, and it makes no sense to minimize the error function Eq. (24) below a threshold value determined by the measurement accuracy $\Delta\Phi$. Thus, we may regard that the minimization was successful when the condition:

$$F < \sum_{i=1}^{M}\sum_{j=1}^{Z} w_i(\omega_j)[\Delta\Phi_{i,\text{measurement}}(\omega_j)]^{2g} \tag{25}$$

is fulfilled. As several sets of optical constants may fulfill Eq. (25), we may obtain a multiplicity of mathematically acceptable solutions, from which the physically meaningful has to be selected. Especially in thin film optics, the discussion of the solution multiplicity may be a troublesome procedure.

If one has no idea on the mutual correlation of the optical constants at different frequencies, one may straightforwardly apply the minimum condition of Eq. (24):

$$\text{grad}_N F = \vec{0} \tag{26}$$

which reduces to a set of Z equation systems:

$$\Phi_{i,\text{theor.}}(N(\omega_j), \omega_j, \ldots) - \Phi_{i,\text{measurement}}(\omega_j) = 0 \tag{27}$$

in the case that no analytical dependence of the optical constants at different frequencies is assumed. These systems of equations may be solved numerically at each frequency of interest, which would be a typical single wavelength procedure.

As a disadvantage, it often suffers from a multiplicity of solutions, especially in thin film systems.

There exist several methods to reduce the solutions multiplicity. First of all, a sufficient number of independent measurements or their clever choice may reduce the solutions' multipicity, however, it demands the access to the corresponding measurement equipment. Occasionally, photometric spectra (e.g., transmittance) are included into Eq. (24) together with ellipsometric data.

However, it is often impossible to increase the number of measurements because of a lack of equipment. One further way to reduce a possible solution multiplicity is given by the application of curve fitting procedures. In this case, one postulates an analytical dispersion law in the form:

$$N(\omega) = f(\omega, p_1, p_2, \ldots) \tag{28}$$

where the p-values represent a set of parameters. As an example, one may use the Cauchy formula:

$$n(\omega) = p_1 + p_2\omega^2 + p_3\omega^4 + \ldots \tag{29}$$

or other well-known approaches, for instance as given by Eq. (19). Then the minimization of F embodies the determination of the p-values, so that as the result we have a formula which defines the (complex) refractive index as a function of frequency.

The curve fitting procedures are widely applied today, however, their successful application demands the reliable choice of a suitable dispersion law as in Eq. (28). One of their advantages is that they may find application in quite restricted spectral regions.

A more general approach is based on the application of the Kramers–Kronig formulae, which may be written as

$$\begin{aligned} \mathrm{Re}\,\epsilon(\omega) &= 1 + \frac{2}{\pi}\int_0^\infty \frac{\xi\,\mathrm{Im}\epsilon(\xi)}{\xi^2 - \omega^2}\,d\xi \\ \mathrm{Im}\,\epsilon(\omega) &= -\frac{2\omega}{\pi}\int_0^\infty \frac{[\mathrm{Re}\,\epsilon(\xi) - 1]}{\xi^2 - \omega^2}\,d\xi + \frac{\sigma_{\mathrm{stat}}}{\epsilon_0\omega} \end{aligned} \tag{30}$$

where σ_{stat} is the static electric conductivity of the material investigated. Equation (30) defines a relation between the frequency response of the real and imaginary parts of the dielectric function. These follow directly from the fundamental requirement that the interaction of light with matter must be consistent with the causality principle. Therefore, if any set of optical constants determined by minimizing Eq. (24) is not Kramers–Kronig consistent, it is physically meaningless and may be excluded.

Equation (30) forms the basis of the Kramers–Kronig methods for determining optical constants. Today, a Kramers–Kronig analysis is often incorporated in modern spectrophotometer operating software. Its only disadvantage is that the integration is accomplished in an infinitively large frequency region, which is not accessible in practice, so that one has to apply extrapolation procedures.

Remarks on Thin Film Spectroscopy

A further complication of the sample's optical description appears when the sample thickness becomes smaller than the coherence length of the light interacting with the sample. In this case, the intensity addition as mentioned in connection with Eq. (18) becomes incorrect, and must be replaced by the addition of the complex field strength values which contain information on both the amplitude and the relative phase of the light. This leads to quite involved mathematical expressions, which will not be presented here—the reader is therefore referred to the literature (12,13,14). The most significant feature of thin film optics is the appearance of interference pattern in the spectra.

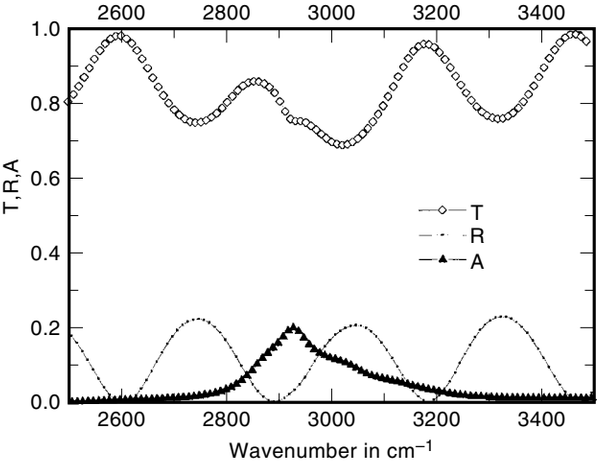

Figure 8. Normal incidence spectra of a 10 μm thick foil, considering the optical constants from Fig. 5 and thin film interferences, as calculated by Eq. (31). The sinusoidal structures in the transmittance prevent a simple identification of absorption lines. Taking the reflectance into account, the absorption may be calculated via Eq. (1), which leads to a more reliable identification of the absorption structure from Fig. 5.

The origin of the interference pattern may be explained in terms of the wave picture of electromagnetic irradiation. If the coherence length of the light is large enough, then the waves reflected from the first and second (or further) interfaces may constructively or destructively interfere with each other, depending on the light wavelength. This will finally lead to characteristic periodic structures in the spectra, as demonstrated below.

As illustration Fig. 8 shows the normal incidence transmittance, reflectance, and absorption calculated for a 10 micrometer thick free-standing foil with the same optical constants as shown in Fig. 5. In contrast to Fig. 6, the calculation has not been performed by Eq. (18) but by the corresponding thin film formulae, which should be written in the present case as

$$\begin{aligned} T &= \left|\frac{t_{12}t_{21}e^{i\beta}}{1 + r_{12}r_{21}e^{2i\beta}}\right|^2; \quad R = \left|\frac{r_{12} + r_{21}e^{2i\beta}}{1 + r_{12}r_{21}e^{2i\beta}}\right|^2; \\ \beta &= 2\pi\upsilon d\sqrt{N_2^2 - \sin^2\varphi}; \end{aligned} \tag{31}$$

Here, d has to be regarded as the film thickness. Equation (31) is more general than Eq. (18); the latter will be obtained when Eq. (31) is averaged over the real part of β (averaged over the phase). The main difference to Fig. 6 is the appearance of sinusoidal structures in transmittance and reflectance spectra, caused by interferences between the two boundaries of the foil. Obviously, a direct identification of the assumed

absorption structure is problematic when only the transmittance is known. However, if the reflectance is also available, the absorption may be calculated via (1) neglecting scattering, and the obtained absorption shows the characteristic features assumed in the absorption coefficient.

Besides spectrophotometry, variable angle spectroscopic ellipsometry (VASE) has become a powerful tool for optical investigation of thin film systems today, especially if it is combined with transmission spectroscopy.

The appearance of an interference pattern in thin film spectra offers the possibility of a simple optical film thickness determination for single film systems, avoiding the minimization of Eq. (24). Indeed, if we know the wavenumbers v_1 and v_2 of two neighboring interference extrema (e.g., in the reflectance shown in Fig. 8), from Eq. (31) it follows immediately that the thickness may be calculated using

$$|v_1 - v_2| = \frac{1}{4d\sqrt{n^2 - \sin^2 \varphi}} \tag{32}$$

in the case that the refractive index is almost real. The refractive index may be determined from the reflectance values achieved in the extrema values of the interference pattern. Optical nondestructive thickness determination is of great practical importance, for example for in situ thickness monitoring of thin solid films during thin film deposition procedures. More details are given in the literature.

Concluding this section, we mention the possibility of combining the reflection spectroscopy (in both photometric and ellipsometric versions) with the excitation of so-called propagating surface plasmon-polaritons (15). In this case, a surface plasmon is optically excited at a metal surface (for example silver), usually by application of so-called grating or prism couplers. The high local electric field of the plasmon polariton may interact with a thin dielectric film or adsorbate located near the metal surface. On this basis, surface sensitive spectroscopy methods have been developed to investigate the properties of the thin film or the adsorbate. They include linear spectroscopy (reflectance, ellipsometry, luminescence, Raman scattering), as well as nonlinear spectroscopy, which needs high electric fields to be efficient in output.

Examples of Linear Laser Spectroscopy

As already mentioned, the measurement of small losses is often performed with lasers as light sources, due to the high intensity of their irradiation. The purpose of this section is to discuss selected versions of linear laser spectroscopy, which are frequently used in material sciences; namely, Raman spectroscopy and laser calorimetry.

Raman Spectroscopy. Scatter losses may be subdivided into elastic and inelastic scatter losses. For elastic scatter losses, the frequency of the scattered light is identical with that of the impinging one. Rayleigh and Mie scattering belong to elastic scattering processes. On the contrary, inelastically scattered light exhibits frequency shifts with respect to the incoming one, and the value of the frequency shift is characteristic for the material illuminated. Therefore, inelastic scattering processes may be used to characterize (or even identify) materials as well as absorption techniques.

Let us start with the case of a crystal. Imagine an electromagnetic wave (the so-called excitation line, in most cases generated by a laser) traveling through the medium. The interaction of the light wave with the phonon modes in the crystal may lead to inelastic scattering of the light wave, resulting in the generation or annihilation of phonons. The latter may be detected through the appearance of new lines in the spectrum, which are red-shifted (Stokes lines, corresponding to phonon generation) or blue-shifted (Antistokes lines, corresponding to phonon annihilation) with respect to the initial laser frequency (the excitation frequency $\omega_{\text{exc.}}$). The intensity ratio between Stokes and Antistokes lines is temperature dependent because of the different thermal population of the phonon states in equilibrium conditions. Depending on the type of phonons which scatter the excitation line, one speaks about Raman scattering (optical phonon modes) or Brillouin scattering (acoustical phonon modes). We will focus on the Raman case.

The frequency of the scattered light is given by

$$\omega_{\text{Raman}} = \omega_{\text{exc.}} \pm m\omega_{\text{Phonon}} \tag{33}$$

where ω_{Raman} is the frequency of the scattered light and ω_{Phonon} is that of the phonons, and m is the order of the Raman process.

Thus, Raman scattering processes give information about the vibrational eigen frequencies of a given material. In Raman spectroscopy, the Raman lines are resolved and used to determine the vibrational eigen frequencies. Due to the higher line intensity, this is usually performed in the Stokes region. In contrast to infrared absorption spectroscopy, in Raman spectroscopy the information is up-converted into another spectral range (usually into the visible), as seen from Eq. (33). Moreover, the Raman selection rules differ from those of infrared absorption, so that for certain classes of materials infrared spectroscopy and Raman spectroscopy are complementary. Equipped with triple monochromators and microscopes, so-called micro-Raman spectrometers combine the advantages of both high frequency and high spatial resolutions and represent thus a powerful tool in optical probe techniques.

As a consequence of momentum conservation in crystals, a first-order Raman spectrum ($m = 1$) can only contain the response of zone-center phonons. This selection rule breaks down in disordered materials.

Laser Calorimetry. We finish our discussion of optical materials characterization with a widely used absorption technique. As already mentioned, in the absence of fast radiative relaxation channels, the light absorption of a sample leads to sample heating, which may be measured. To detect small absorption losses, a laser beam is directed on the sample, which leads to a sample temperature increase according to

$$P_A = C\frac{\Delta T_s}{\Delta t} \tag{34}$$

where P_A is the absorbed power, t is time, C is the sample heat capacity, and T_s the sample temperature (do not confuse with the transmittance). An instantaneous measurement of

the transmitted (P_T) and reflected (P_R) powers leads to the absorptance via

$$A = \frac{P_A}{P_A + P_T + P_R}, \tag{35}$$

when scatter losses are negligible. In practice, all the power values are averaged over the light exposure time. Having determined the sample absorptance, the absorption coefficient may principally be calculated performing a reverse search [minimization of Eq. (24)]. For simple geometries (uncoated wafer as in Fig. 2, normal light incidence), the absorption coefficient may be estimated via

$$\alpha \approx \frac{A}{d} \tag{36}$$

where d is the wafer thickness. As laser calorimetry provides a direct absorptance measurement, it allows one to record absorption values many orders of magnitude below that which may be achieved by means of spectrophotometry.

BIBLIOGRAPHY

1. M. Born and E. Wolf, *Principles of Optics,* Oxford: Pergamon Press, 1980.
2. H. K. Pulker, Characterization of optical thin films, *Appl. Opt.,* **18**: 1979, 1969–1977.
3. H. Kuzmany, *Festkörperspektroskopie,* Berlin: Springer-Verlag, 1990.
4. John Daintith (ed.), *The Facts on File-Dictionary of Physics,* revised and expanded edition, New York: Facts on File Inc., 1988.
5. L. D. Landau and E. M. Lifschitz, *Lehrbuch der theoretischen Physik, Band VIII: Elektrodynamik der Kontinua,* Berlin: Akademie-Verlag, 1985.
6. P. Klocek (ed.), *Handbook of Infrared Optical Materials,* New York: Marcel Dekker, Inc., 1991.
7. M. Schubert and B. Wilhelmi, *Einführung in die nichtlineare Optik II,* BSB B.G.Teubner, Verlagsgesellschaft Leipzig, 1978.
8. N. Bloembergen, *Nonlinear Optics,* Reading, MA: Addison-Wesley, 1992.
9. O. Stenzel, *Das Dünnschichtspektrum: Ein Zugang von den Grundlagen zur Spezialliteratur,* Berlin: Akademie-Verlag, 1996.
10. W. Demtröder, *Laser Spectroscopy-Basic Concepts and Instrumentation,* Berlin: Springer-Verlag, 1996.
11. J. H. Dobrowolski, F. C. Ho, and A. Waldorf, Determination of optical constants of thin film coating materials based on inverse synthesis, *Appl. Opt.,* **22**: 1983, 3191–3200.
12. D. P. Arndt et al., *Appl. Opt.,* **23**: 1984, 3571–3596.
13. M. R. Jacobson (ed.), Selected papers on characterization of optical coatings, Milestone Series v. **MS63**: SPIE Optical Engineering Press, 1992.
14. O. Stenzel and R. Petrich, Flexible construction of error functions and their minimization: Application to the calculation of optical constants of absorbing or scattering thin-film materials from spectrophotometric data, *J. Phys. D: Appl. Phys.,* **28**: 978–989, 1995.
15. H. Raether, *Surface plasmons on smooth and rough surfaces and on gratings,* Tracts in Modern Physics 111, Berlin: Springer-Verlag, 1988.

OLAF STENZEL
ALEXANDER STENDAL
Technische Universität Chemnitz